Clinical Cancer Research

The Genomic Landscape of Merkel Cell Carcinoma and Clinicogenomic Biomarkers of Response to Immune Checkpoint Inhibitor Therapy

Todd C. Knepper[1], Meagan Montesion[2], Jeffery S. Russell[3], Ethan S. Sokol[2], Garrett M. Frampton[2], Vincent A. Miller[2], Lee A. Albacker[2], Howard L. McLeod[1], Zeynep Eroglu[4], Nikhil I. Khushalani[4], Vernon K. Sondak[4], Jane L. Messina[5], Michael J. Schell[6], James A. DeCaprio[7], Kenneth Y. Tsai[5,8,9], and Andrew S. Brohl[4,10]

Abstract

Purpose: Merkel cell carcinoma (MCC) is a rare, aggressive cutaneous malignancy, which has demonstrated sensitivity to immune checkpoint inhibitor therapy. Here, we perform the largest genomics study in MCC to date to characterize the molecular landscape and evaluate for clinical and molecular correlates to immune checkpoint inhibitor response.

Experimental Design: Comprehensive molecular profiling was performed on 317 tumors from patients with MCC, including the evaluation of oncogenic mutations, tumor mutational burden (TMB), mutational signatures, and the Merkel cell polyomavirus (MCPyV). For a subset of 57 patients, a retrospective analysis was conducted to evaluate for clinical and molecular correlates to immune checkpoint inhibitor response and disease survival.

Results: Genomic analyses revealed a bimodal distribution in TMB, with 2 molecularly distinct subgroups. Ninety-four percent ($n = 110$) of TMB-high specimens exhibited an ultraviolet light (UV) mutational signature. MCPyV genomic DNA sequences were not identified in any TMB-high cases (0/117), but were in 63% (110/175) of TMB-low cases. For 36 evaluable patients treated with checkpoint inhibitors, the overall response rate was 44% and response correlated with survival at time of review (100% vs. 20%, $P < 0.001$). Response rate was 50% in TMB-high/UV-driven and 41% in TMB-low/MCPyV-positive tumors ($P = 0.63$). Response rate was significantly correlated with line of therapy: 75% in first-line, 39% in second-line, and 18% in third-line or beyond ($P = 0.0066$). PD-1, but not PD-L1, expression was associated with immunotherapy response (77% vs. 21%, $P = 0.00598$, for PD-1 positive and negative, respectively).

Conclusions: We provide a comprehensive genomic landscape of MCC and demonstrate clinicogenomic associates of immunotherapy response.

Introduction

Merkel cell carcinoma (MCC) is a rare and deadly neuroendocrine malignancy of the skin with variable incidence across geographic regions correlated with exposure to UV radiation, a known risk factor for the disease (1–4). In 2008, the Merkel cell polyomavirus (MCPyV) was discovered and is now considered the most common etiologic agent of MCC (5–7). The discovery of the MCPyV spurred interest in uncovering prognostic differences and optimizing treatment strategies between virus-positive and virus-negative patients (8–10).

Historically, prognosis for patients with advanced MCC was poor, with less than 20% alive at 5 years (11–14). Although first described in 1972 (15), there were no FDA-approved treatments for patients with MCC prior to the approval of avelumab, an anti-PD-L1 checkpoint inhibitor, in March 2017. MCC is sensitive, at least in the short term, to chemotherapeutics including platinum agents and etoposide, with first-line response rates of 53% to 61% (16–20).

Recently, the treatment paradigm for advanced MCC has shifted dramatically, with immune checkpoint inhibitors demonstrating remarkable efficacy in this disease. In the first-line setting, a single-arm study of pembrolizumab in 26 patients with

[1]Department of Individualized Cancer Management, H. Lee Moffitt Cancer Center and Research Institute, Tampa, Florida. [2]Foundation Medicine, Inc., Cambridge, Massachusetts. [3]Janssen Pharmaceuticals, Inc., Springhouse, Pennsylvania. [4]Department of Cutaneous Oncology, H. Lee Moffitt Cancer Center and Research Institute, Tampa, Florida. [5]Department of Anatomic Pathology, H. Lee Moffitt Cancer Center and Research Institute, Tampa, Florida. [6]Department of Biostatistics and Bioinformatics, H. Lee Moffitt Cancer Center and Research Institute, Tampa, Florida. [7]Department of Medical Oncology, Dana-Farber Cancer Institute, Boston, Massachusetts. [8]Department of Tumor Biology, H. Lee Moffitt Cancer Center and Research Institute, Tampa, Florida. [9]Department of Chemical Biology and Molecular Medicine, H. Lee Moffitt Cancer Center and Research Institute, Tampa, Florida. [10]Sarcoma, H. Lee Moffitt Cancer Center and Research Institute, Tampa, Florida.

Note: Supplementary data for this article are available at Clinical Cancer Research Online (http://clincancerres.aacrjournals.org/).

T.C. Knepper and M. Montesion contributed equally to this article.

Corresponding Authors: Andrew S. Brohl, H. Lee Moffitt Cancer Center and Research Institute, Tampa, FL 33612. Phone: 813-745-3242; E-mail: andrew.brohl@moffitt.org; and Kenneth Y. Tsai, Kenneth.tsai@moffitt.org

Clin Cancer Res 2019;25:5961–71

doi: 10.1158/1078-0432.CCR-18-4159

Translational Relevance

This is the largest genomics study of Merkel cell carcinoma (MCC) to date, providing a comprehensive landscape of recurrent driver mutations and highlighting the molecular distinction between the ultraviolet light (UV)-driven and viral-driven subtypes. We further evaluate clinicogenomic markers of immunotherapy response in a large institutional cohort. Response rates to checkpoint inhibitor therapy are highest when used first line, and the genomic relationship to other cancers suggests that differential therapeutic strategies may be appropriate for each subtype despite similar responses to immunotherapy. PD-1, but not PD-L1 expression, was associated with favorable immunotherapy response. These results provide a comprehensive genomic characterization of MCC, show a novel means of detecting MCPyV using targeted sequencing, place molecular subgroups in the context of other human cancers, and demonstrate the importance of using immunotherapy as early as possible.

MCC demonstrated response rates of 62% and 44% in MCPyV-positive and MCPyV-negative cases, respectively (21). In the setting of previous chemotherapy treatment, a single-arm study of avelumab in 88 patients demonstrated an overall response rate of 33% (26.1% and 35.5% in MCPyV-positive and MCPyV-negative cases, respectively; ref. 22). This study led to the accelerated approval of avelumab for the treatment of patients with metastatic MCC, the first FDA approved therapy for the disease. Updated avelumab efficacy analysis showed that responses were durable, with an estimated 74% of responses lasting $\geq$1 year (median duration not reached), and with 1-year PFS and overall survival (OS) rates of 30% and 52% respectively, for the entire cohort (23). Updated pembrolizumab efficacy data have similarly demonstrated favorable durability of responses and survival rates (24). Although these studies assessed the impact of biomarkers such as viral status and PD-L1 status on efficacy, no subgroup has been reliably established as conferring a statistically significant difference. Thus, there remains an ongoing search for biomarkers to predict response.

With the advent of next-generation sequencing (NGS), the mutational profile of MCC has emerged. MCPyV-positive and MCPyV-negative MCC's have displayed unique mutational profiles. For MCPyV-negative patients, NGS and whole exome sequencing have revealed a high tumor mutational burden (TMB), with recurrent mutations in *TP53* and *RB1*. On the other hand, for MCPyV-positive patients a particularly low TMB has been noted, without a pattern of recurrent mutations (25–29). Because of the rarity of MCC, comprehensive genomic analyses have been limited studies of less than 50 patients. Furthermore, there is an even greater paucity of information from comprehensive genomic analyses in tandem with clinical correlation, including the association between genomics and response to therapy.

In this study, comprehensive genomic profiling on MCC tumors from 317 patients was performed to characterize the genomic landscape of MCC. In addition, a retrospective clinical and genomic analysis via NGS of 57 consecutive patients diagnosed with MCC was conducted at a single academic cancer center. The objective was to evaluate both clinical and molecular correlates to immunotherapy response and patient survival.

Materials and Methods

Study design and participants

Assessment of genomic landscape (Full Genomic Cohort) included all patients ($n = 317$) with a reported diagnosis of MCC who underwent comprehensive genomic profiling by Foundation Medicine between May 2013 and April 2018. For the clinical portion of this study (Clinical Cohort), a retrospective, single-center analysis was performed for all consecutive patients diagnosed with advanced/metastatic MCC and treated at Moffitt Cancer Center who underwent comprehensive genomic profiling by Foundation Medicine between September 2014 and August 2017. A retrospective chart review collected demographic, clinical, disease, treatment, and outcome variables on 57 patients, all of whom are included in the larger 317 patient genomic analysis. Patients were considered responders if they were assessed as having a complete response (CR), partial response (PR), or stable disease for at least 6 months by the treating physician. This study was approved under IRB protocol MCC #19191 (Pro00022458) at Moffitt Cancer Center and the Western Institutional Review Board (Protocol No. 20152817) at Foundation Medicine, Inc. Although the diagnosis of MCC is supported for the cases on the clinical portion as detailed below, the diagnosis of MCC for the remaining cases were reported from the requesting institution to Foundation Medicine and could not be independently verified histopathologically. The study was performed in accordance with the ethical guidelines of the Belmont report. Where required, written consent was obtained from study subjects.

Sequencing and genomic analysis

Comprehensive genomic profiling of 322 unique cancer-related genes, including evaluation of TMB and mutational signatures, was performed on MCC tumors from 317 patients. DNA ($\geq$50 ng) was extracted from formalin-fixed paraffin-embedded (FFPE) specimens' archival tissue and sequenced to a median coverage depth of 500$\times$ using a hybrid capture-based NGS platform that covers the entire coding region of 315 cancer-related genes and select introns from 28 genes that are commonly rearranged or altered in cancer (FoundationOne). All NGS was performed in a Clinical Laboratory Improvement Amendments (CLIA)-certified, College of American Pathologists (CAP)-accredited, New York State approved laboratory (Foundation Medicine). Genomic data were analyzed for point mutations, short insertions and deletions, copy number alterations, rearrangements, and TMB as part of routine clinical care. TMB was calculated as the number of nondriver somatic coding mutations per megabase of genome sequenced. The categories of TMB-low (<6 mutations/MB), TMB-intermediate (6–19 mutations/MB), and TMB-high ($\geq$20 mutations/MB) are based on those used in the FoundationOne assay (30–32).

Mutational signatures

Mutational signatures were determined in all samples containing at least 20 nondriver somatic missense alterations, including silent and noncoding mutations. Signatures were assigned by analysis of the trinucleotide context and profiled using the Sanger COSMIC signatures of mutational processes in human cancer, as described by Zehir and colleagues (33). A positive status was determined if a sample had at least a 40% fit to a mutational process, as is convention (33). The COSMIC UV signature

(signature 7) is dominated by C>T transition mutations in a CC or TT dinucleotide context (34).

MCPyV detection

Presence of MCPyV was detected through DNA sequences consistent with genomic MCPyV DNA. Specifically, determined through Velvet *de novo* assembly of off-target sequencing reads left unmapped to the human reference genome (hg19). Assembled contigs were competitively aligned by BLASTn to the NCBI database of all known viral nucleotide sequences (3.6 million sequences total, 574 of which were MCPyV-specific). Positive viral status was determined by contigs $\geq$100 nucleotides in length and with $\geq$98% identity to the BLAST sequence. MCPyV integration sites were determined using discordant read pairs where one read aligned to a location within the human reference genome (hg19) and one read aligned to the MCPyV reference genome (NC_010227.2 MCPyV isolate R17b, complete genome; Supplementary Fig. S1). A positive integration site was determined if the majority of human reads aligned to one genomic region, with at least 2 reads mapping. Additional viral analysis was performed by IHC in 36 of the clinically annotated cases for which materials were available. IHC for viral antigens was performed at the Dana Farber Cancer Institute using the CM2B4 and MCV203Ab3 antibodies for 22 cases and MCV203Ab3 for 14 subsequent cases given complete concordance between initial results obtained from the 2 antibodies. The CM2B4 antibody had some false-positive reactivity manifested as faint nuclear staining of lymphocytes. Mouse monoclonal antibodies MCV203Ab3 and CM2B4 (Santa Cruz Biotechnology Inc.) were applied at the indicated final concentration (0.6 or 2.4 μg/mL for MCV203Ab3; 2 μg/mL for CM2B4) in Dako diluent for 1 hour.

Clustering and gene enrichment analyses

Clustering and gene enrichment analyses were performed on 18 selected tumor types sequenced by the FoundationOne assay. Clustering was achieved by comparing the prevalence of the top 10 most frequently altered genes within each tumor type and clustered based on Euclidean distance. To investigate which genes were driving the clustering seen between the TMB-high MCC samples and other neuroendocrine tumors (prostate neuroendocrine carcinoma, bladder neuroendocrine carcinoma, and small cell lung carcinoma), a gene enrichment analysis was performed by comparing the genomic alterations detected in these samples against the genomic alterations detected in the other tumor types. The odds ratios and *P* values were determined using Barnard's test.

PD-L1 and PD-1 expression

Dual IHC for PD-L1 and PD-1 expression was performed using Cell Signaling Technologies #13684 (clone E1L3N) and Abcam AB52587 (Nat105) in the Tissue Core Facility at Moffitt Cancer Center and evaluated on 37 cases total and 27/36 cases with evaluable responses to immunotherapy (Supplementary Fig. S2). PD-L1 expression was quantified using manual morphometric analysis in blinded fashion by a dermatopathologist (KYT). Given the large variability of tissue sample sizes, the following approach was used. PD-L1 expression was largely confined to the tumor periphery and quantitated on the basis of estimating the proportion of tumor cells expressing membranous or membranous and cytoplasmic PD-L1. The tumor periphery was defined here as the 50-μm-thick outer edge of every physically distinct tumor nodule. Within this region, the proportion of tumor cells exhibiting expression was quantitated as <1% (negative) or $\geq$1% (positive). All evaluated tumors had some expression of PD-L1.

Because of the relative paucity of PD-1 expression overall, the staining was scored solely on the basis of presence (1) or absence (0) of expression on peritumoral (within 0.02 mm = 20 μm of tumor periphery) lymphocytes (35).

Statistical analysis

Summary statistics are descriptive for demographics, clinical characteristics, and treatment patterns. For continuous data, medians and interquartile ranges (IQR) are presented. For categorical data, frequencies and percentages are presented. No adjustments were made for multiplicity. Statistical analyses were done with SAS software, version 9.3.

OS was analyzed using the Kaplan–Meier method to compare the survival of immunotherapy responders versus those with progressive disease. A univariate analyses using the Barnard test was used to generate *P* values for the relationships between immunotherapy response and molecular subtype, PD-L1 status and PD-1 status. A Mantel–Haenszel test was used to detect a linear association between line of immunotherapy treatment and response. Barnard test was utilized to calculate *P* values for the remaining comparisons (36).

Role of the funding source

The funders of the study had no role in the study design, data collection, data analysis, data interpretation, or the writing of the report. TCK, ASB, and KYT had full access to all the data from the clinical cohort and MM had full access to all the data from the genomic cohort. Foundation Medicine provided data generated through the genomic analyses that they performed in the commercial setting but did not provide a direct financial contribution to support or influence this study. JSR's role in conducting this study predated his employment by Janssen Pharmaceuticals, Inc., and no financial contribution was made to this study by Janssen Pharmaceuticals, Inc.

Results

The baseline demographics of the patients in this study were consistent with those reported in previous studies of this disease. The male:female prevalence was approximately 4:1 in both the full genomic group and the Moffitt subgroup ("clinical cohort"). The median age (years) at sequencing was 71 (IQR = 63–78) for the full genomic cohort ($n = 317$) and the median age at time of sequencing biopsy was 73 (IQR = 66–80) for the clinical cohort ($n = 57$). In the clinical cohort, the vast majority of patients were non-Hispanic Caucasians (98%) and had been diagnosed with advanced stage MCC (stage IIIB or IV) by the time of sequencing biopsy (45/57, 79%; Table 1). Forty-nine of 53 cases evaluated for CK20 expression were CK20-positive with the characteristic perinuclear accentuation. The 4 CK-20 negative cases all had pan-cytokeratin expression with characteristic perinuclear accentuation, with additional markers such as synaptophysin, CD56, and/or AE1/AE3. Two-thirds ($n = 38$, 67%) of patients in the clinical cohort received treatment with an immune checkpoint inhibitor by the time of data cutoff for the chart review, 36 of whom were assessable for response. The most common immune checkpoint therapies utilized were pembrolizumab ($n = 18$,

Table 1. Baseline characteristics and treatment data for patients in retrospective analysis

Characteristic	Value
Baseline characteristics ($n = 57$)	
Age (years)	
At diagnosis, median (range)	71 (29–88)
At biopsy, median (range)	73 (29–88)
At sequencing, median (range)	73 (30–88)
Sex	
Male	46 (81%)
Female	11 (19%)
Race	
Caucasian	57 (100%)
Ethnicity	
Non-Hispanic	56 (98%)
Hispanic	1 (2%)
Stage at biopsy	
I	2 (4%)
I or II	1 (2%)
II	2 (4%)
IIIA or IIIB	7 (12%)
IIIB	11 (19%)
IV	34 (60%)
Immunocompromised	
No	51 (89%)
CLL	2 (4%)
Transplant	2 (4%)
Lupus	1 (2%)
Rheumatoid arthritis	1 (2%)
Treatment data for immunotherapy-treated patients ($n = 38$)	
Immunotherapy received	
Pembrolizumab	18 (47%)
Avelumab	10 (26%)
Pembrolizumab; ipilimumab + nivolumab	3 (8%)
Pembrolizumab; avelumab	3 (8%)
Avelumab; pembrolizumab	2 (5%)
Ipilimumab + nivolumab	1 (3%)
Nivolumab	1 (3%)
Line of therapy when immunotherapy first received	
1	12 (32%)
2	15 (40%)
3	6 (16%)
4	3 (8%)
5	2 (5%)
Radiation sequence relative to immunotherapy	
Radiation first	30 (79%)
Immunotherapy first	2 (5%)
No radiation	6 (16%)
Immunotherapy treatment follow-up (months)	
Median (range)	12.1 (0.6–33.2)

NOTE: Data are *n* (%) unless stated otherwise. Total percentage values might sum to >100% because of rounding. CLL, chronic lymphocytic leukemia.

47%), avelumab ($n = 10$, 26%), nivolumab ($n = 1$, 2%), and ipilimumab plus nivolumab ($n = 1$, 2%). Five patients (13%) received sequenced avelumab and pembrolizumab, with pembrolizumab first followed by avelumab in 3 cases, and the reverse in 2. Of the patients who received any immunotherapy, the initial treatment with checkpoint inhibitor was received in the first line for 12 patients (32%), the second line for 15 (39%), and in the third or later line for 11 (29%). Thirty (79%) of the patients treated with immunotherapy received prior radiation therapy, the remaining 8 patients either did not receive radiation ($n = 6$) or underwent radiation therapy at some point after immunotherapy treatment ($n = 2$; Table 1).

Genomic analysis revealed that the TMB of MCC exhibited a bimodal distribution between TMB-high and TMB-low specimens, with only 25 (8%) specimens having an intermediate TMB (Fig. 1A). Overall, 117/317 (37%) of MCC samples were TMB-high (median = 53.9 mutations/MB; range = 20.4–217.5; IQR = 40.9–70.9) and in contrast, 175/317 (55%) of MCC specimens were TMB-low (median = 1.2 mutations/MB; IQR = 0.0–2.6). Within the clinical cohort the trend was the same, with only 5% (3/57) patients having an intermediate TMB, whereas 39% (22/57) were TMB-high (median = 63.1; range = 31.3–133.1 mutations/MB; IQR = 46.3–75.9), and the remaining 56% (32/57) TMB-low. *TP53* and *RB1* were the 2 most frequently mutated genes in both the TMB-high and TMB-low groups, but the proportion of cases carrying mutations in those genes were drastically different (Fig. 1C and D). All (117/117, 100%) TMB-high cases had a short variant mutation in either *TP53* or *RB1* or both, whereas 40% (70/175) of the TMB-low cases had no genomic alteration that is known or likely to be an oncogenic driver in any gene within the Foundation panel. Overall, the top altered genes in the TMB-low cohort included *TP53* (13%), *RB1* (9%), and *PTEN* (7%). In contrast, the top altered genes in the TMB-high cohort included *TP53* (97%), *RB1* (80%), NOTCH family (50%; [*NOTCH1* (45%), *NOTCH2* (14%), *NOTCH3* (6%), *NOTCH4* (4%)]), *KMT2D* (26%), *FAT1* (26%), *LRP1B* (23%), *PIK3CA* (21%), *TERT* (15%), and *KMT2C* (13%). In addition, we report a number of recurrently mutated genes at lower frequencies (Supplementary Table S1). Copy number alterations were detected in only 24% (28/117) of the TMB-high specimens. Copy number gains were restricted to 2 genes, *MYCL* (7/117, 6%) and *MYC* (5/117, 4%), which were amplified in a mutually exclusive manner, and copy number deletions were detected in 5 genes: *RB1* (5/117, 4%), *PTEN* (2/117, 2%), *TP53* (1/117, 1%), *LRP1B* (1/117, 1%), *CDKN2A* (1/117, 1%), and *NF1* (1/117, 1%).

TMB classification was strongly associated with the presence of MCPyV genomic DNA, which was detected in 36% (114/317) of the overall patient population, including 37% (21/57) of the clinical cohort. MCPyV DNA was not detected in any of the TMB-high cases (0/117), but was detected in 63% (110/175; $P \leq 0.00001$, Barnard test) of the TMB low cohort. The UV damage mutational signature was mutually exclusive with DNA evidence of MCPyV integration but strongly positively correlated with TMB-high classification (Fig. 1B). Ninety-four percent (110/117) of the TMB-high samples expressed a UV signature; classification of mutational signatures required at least 20 nondriver somatic mutations; thus, the TMB-low cases could not be defined by any mutational signature. Of the TMB-intermediate cases, 36% (9/25) were found to have a UV signature and 16% (4/25) were found to be viral-positive by NGS, always in a mutually exclusive pattern. Forty-four percent (11/25) of the TMB-intermediate cases had neither a UV signature nor virus detected, thus were unable to be categorized into one of the 2 molecular subgroups (Fig. 2A; Supplementary Fig. S3). A *post hoc* pooling of the collective mutations in the TMB-low group, resulting in 595 mutations for the entire 175 TMB-low samples, was conducted to allow for mutational signature analysis on the entire cohort. No signature reached the 40% threshold needed to be classified as dominant. The highest match was a 30.1% fit to Signature 5, a nonspecific signature seen across cancer types, followed by Signature 3 (27.5%) and Signature 1 (17.8%). By comparison, there was a 1.1% fit to Signature 2 and a 0% fit to Signature 13, both of which are linked to APOBEC (33, 34) and a 4.2% fit to Signature 7 (UV; Supplementary Fig. S4).

To validate NGS-based viral detection, viral expression by IHC was performed on 36 cases from the clinical cohort, 15 of which

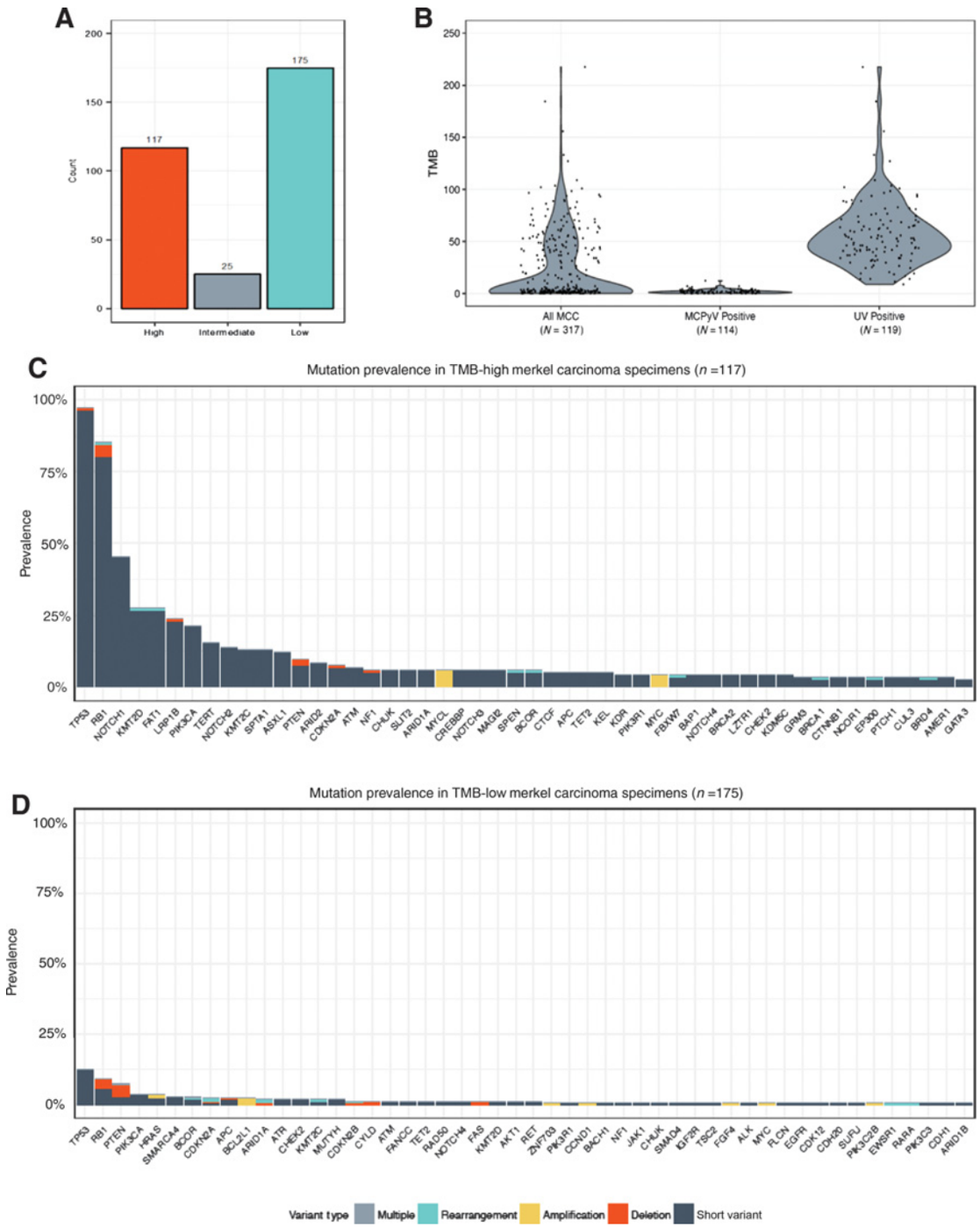

Figure 1.

Genomic landscape of MCC. **A,** Distribution of MCCs with high, intermediate, and low TMB ($N = 317$). **B,** Violin plots of the TMB distribution for the entire cohort and by molecular subgroup; the widest point occurs at the TMB with the largest number of samples. Genes most frequently affected by putatively pathogenic mutation in TMB-high MCC (**C**) and TMB-low MCC (**D**).

were viral-positive and 21 were viral-negative by NGS. MCPyV was detected by IHC in 14/15 (93%) of NGS-positive cases and in 3/21 (14%) of the NGS-negative cases. Of note, all 3 cases that were IHC-positive but NGS-negative were in tumors of low mutational burden. All 15 cases that were NGS-positive were in tumors of low mutational burden (Supplementary Table S2). Of the 114 samples with NGS-detected MCPyV, 7% (8/114) had integration sites identified through discordant viral-human

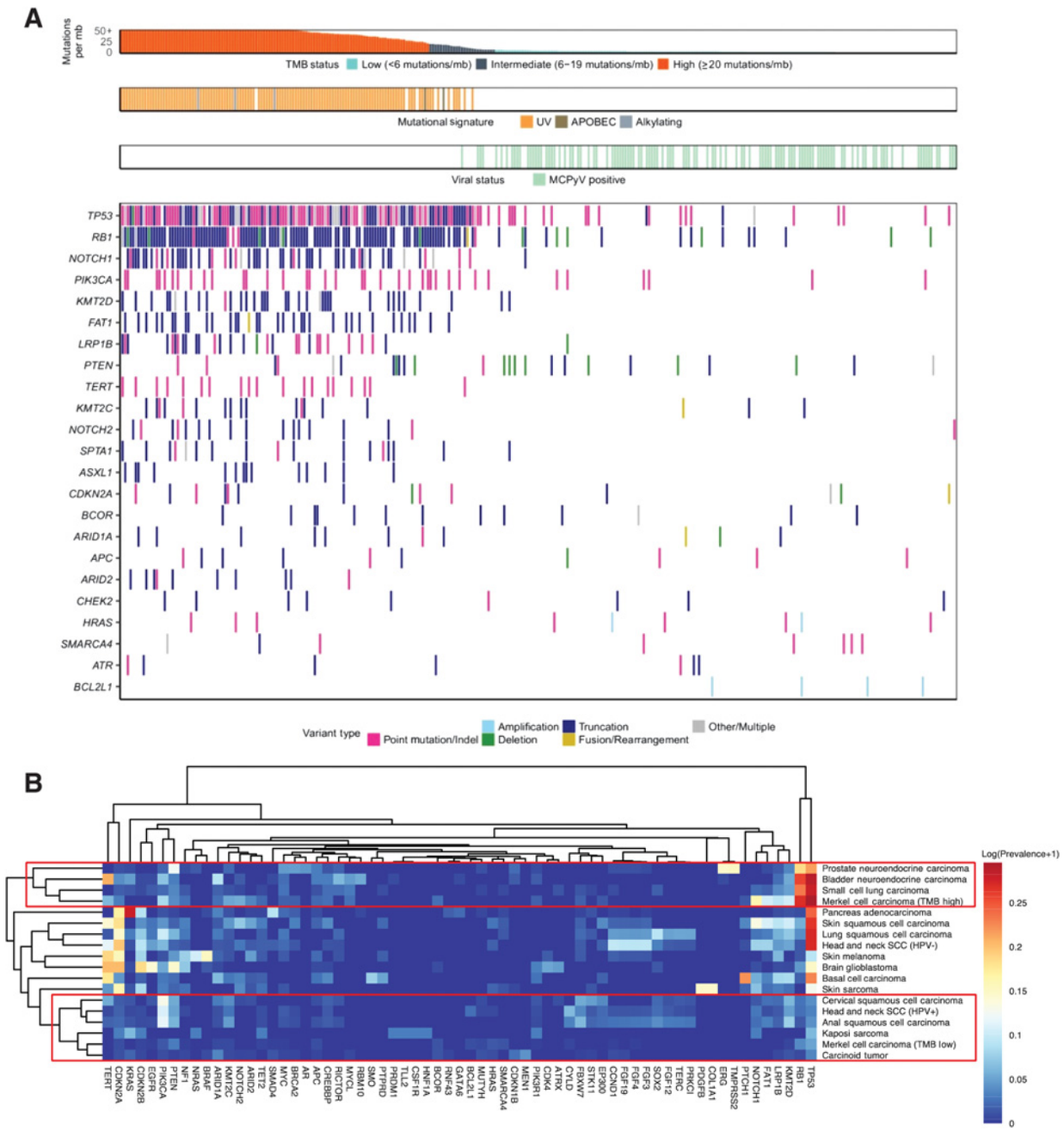

Figure 2.

Molecular subtypes of MCC. **A,** Oncoprint of co-occurrence of TMB status, dominant mutational signature, viral status, and altered gene demonstrating mutual exclusivity of MCV integration and UV damage. Each column corresponds to one unique MCC specimen. Only alterations that are known or likely to be oncogenic are included. Tumors are sorted in descending order by TMB from the left. **B,** Clustering of prevalence of recurrent gene alterations in selected tumor types show that molecular subgroups of MCC cluster separately as compared with other tumor types. The TMB-high subgroup clusters primarily with other neuroendocrine tumor types. The TMB-low subgroup clusters primarily with other viral-driven tumor histologies.

sequencing reads. Of these samples, one integration site appeared to be intergenic while the other 7 sites were located in genes predominantly known to have oncogenic or tumor suppressive functions. Five specimens had integration sites detected within exons (impacted genes: *TP53*, *TOP2A*, *KDM6A*, *CASZ1*, and *PLPPR3*) and 2 specimens had integration sites detected within introns (impacted genes: *LGALS4* and *MICALL2*).

In order to gauge genomic similarity of MCC to other cancers, we performed clustering analysis based upon the ten most commonly altered genes in each of a variety of cancer

types. Surprisingly, TMB-high MCC was most similar to other neuroendocrine cancers such as prostate neuroendocrine carcinoma, bladder neuroendocrine carcinoma, and small cell lung cancer and not UV-associated skin cancers such as squamous and basal cell carcinomas, and melanoma. Indeed, small cell lung cancer (SCLC) is regarded as a close histologic mimic of MCC and typically must be excluded in the routine histopathologic diagnostic evaluation of MCC. Genomic analysis of SCLC reveals a near-universal requirement for loss of *RB1* and *TP53*, with the prevailing notion that loss of NOTCH signaling is important for the neudoendocrine phenotype (37). Although mutations in *KMT2C/D* are common in MCC and are more similar in frequency to cutaneous SCC (38–42), epigenetic modifiers are frequently affected in SCLC, and both MCC and SCLC appear to exhibit altered signaling that appears to converge, at least in part, on *PIK3CA* (37). Likewise, the mutational landscape of neuroendocrine variants of bladder and prostate carcinoma are dominated by *RB1* and *TP53* inactivation (43, 44).

On the other hand, TMB-low MCC was most similar to carcinoid tumors, another rare neuroendocrine tumor, as well as other virally-driven cancers including HPV-positive head and neck squamous cell carcinoma, cervical squamous cell carcinoma, anal squamous cell carcinoma, and Kaposi sarcoma (Fig. 2B). Gene enrichment analysis revealed that 9 genes were significantly enriched in neuroendocrine malignancies, led by *RB1* and *MYCL*, and 6 genes were significantly enriched in non-neuroendocrine malignancies, led by *CDKN2A* and *CDKN2B* and consistent with previous reports of Merkel cell oncogenesis (Supplementary Table S3; refs. 45, 46).

Of the 38 patients in the clinical cohort who received treatment with at least one immune checkpoint inhibitor, 36 were evaluable for response at the time of review. The overall response rate was 44% (16/36). There was a difference in OS between immunotherapy responders and those with progressive disease. All 16 responders were alive with a median follow-up time of 16·9 months from the time of advanced/metastatic diagnosis (IQR = 14.0–27.3), compared with only 20% (4/20) of patients who did not have a favorable response to immunotherapy (median follow-up = 14.8 months; IQR = 9.8–19.5; $P < 0.0001$; Fig. 3A). All responses were classified as either CR (5/36; 14%) or PR (11/36; 31%); with no patients experiencing prolonged stable disease.

For analysis of correlates of immune response, patients were classified by molecular subtype as either UV signature/TMB-high ($n = 14$) or viral positive/TMB-low ($n = 22$; 2 TMB-intermediate patients had a UV signature and did not have MCPyV DNA detected, thus were grouped with TMB-high/UV signature). There was no observed difference in response rate between molecular subgroups, with 50% (7/14) vs. 41% (9/22; $P = 0.63$, Barnard test) responding in the UV versus MCPyV-positive/TMB-low groups, respectively (Fig. 3B; Supplementary Table S4). For other potential correlates of immunotherapy response, a dramatic effect of line of systemic therapy on response was noted (Table 2). The response rate was 75% (9/12) in the first-line setting, 39% (5/13) in the second, and 18% (2/11) when used in third line or beyond ($P = 0.0066$, CMH trend test). Of note, for the 5 patients who received 2 different immunotherapy regimens, only the first regimen utilized was considered for line of therapy analysis. In multivariate analysis including line of therapy, molecular subtype, age, immunosuppression, and prior radiation therapy, line of therapy remained statistically significantly associated with treatment response ($P < 0.01$).

Of the 5 patients who received pembrolizumab and avelumab sequentially, all responses were concordant. One patient achieved a response to both (CR on avelumab, eventually coming off treatment due to grade 3 ALT elevation, followed by on a second CR to pembrolizumab rechallenge after development of a new metastasis) whereas none of the other 4 patients achieved a response to either agent.

Of 6 documented immunocompromised patients within the clinical cohort, 3 were treated with immunotherapy, and 2 of the 3 (one with a renal transplant and another with chronic lymphocytic leukemia) achieved responses. Of note, the patient with renal transplant lost the allograft and required renal replacement therapy as a result of immunosuppression withdrawal and checkpoint inhibitor treatment.

To evaluate the immune microenvironment, IHC for PD-L1 and PD-1 expression was performed in a subset of 27 evaluable patients with available tissue (Table 2). No association between PD-L1 status and immunotherapy response was detected, with a response rate of 54% (7/13) in PD-L1 negative and 43% (6/14) in PD-L1 positive tumors ($P = 0.606$). However, there was a statistically significant association between PD-1 status and response rate, with 10 of 13 (77%) of patients with PD-1 positive tumors responding compared with 3 of 14 (21%) of PD-1 negative ($P = 0.00598$).

Discussion

In this study, we comprehensively characterize 2 molecularly distinct subtypes of MCC, demonstrate the ability of clinically available NGS to accurately distinguish them, and place the molecularly subtypes in the context of other human cancers (Fig. 2B). We perform a retrospective evaluation of clinicogenomic associates to immunotherapy response and show that while both subsets respond similarly well to immunotherapy, clinical response is associated with a long-term impact on survival. Importantly, the use of other therapies prior to immunotherapy negatively influences the ultimate response to immunotherapy, suggesting that immune checkpoint blockade should be used initially when possible.

Prior to this study, the largest genomic analyses of patients with MCC have been performed in fewer than 50 patients, thus limiting the ability to describe less frequent drivers and to cluster molecular subsets (25–29). The magnitude of this study provides a more definitive landscape of the disease, demonstrating the distinctive mutational spectra of MCPyV-positive/TMB-low and UV-driven MCC subgroups (25–27). Although *TP53* and *RB1* rank as the 2 most common mutations in both subsets, the UV-driven subset harbors mutations in genes such as *KMT2C/D*, *FAT1*, and *LRP1B* at high frequency, akin to cutaneous squamous cell carcinoma (38–42, 47). This may imply that MCPyV genes confer the same oncogenic properties as the suite of mutations enriched in the UV-driven subset. Conversely, the frequency of *PTEN* alterations is similar across both subsets, suggesting a common requirement for alterations in this key pathway.

Importantly, the size of our cohort and depth of our profiling enables us to place these 2 classes of MCC within the greater genomic context of human cancers. As a whole, neuroendocrine carcinomas exhibit aggressive clinical behavior with the treatment-emergent variant of neuroendocrine prostate cancer arising

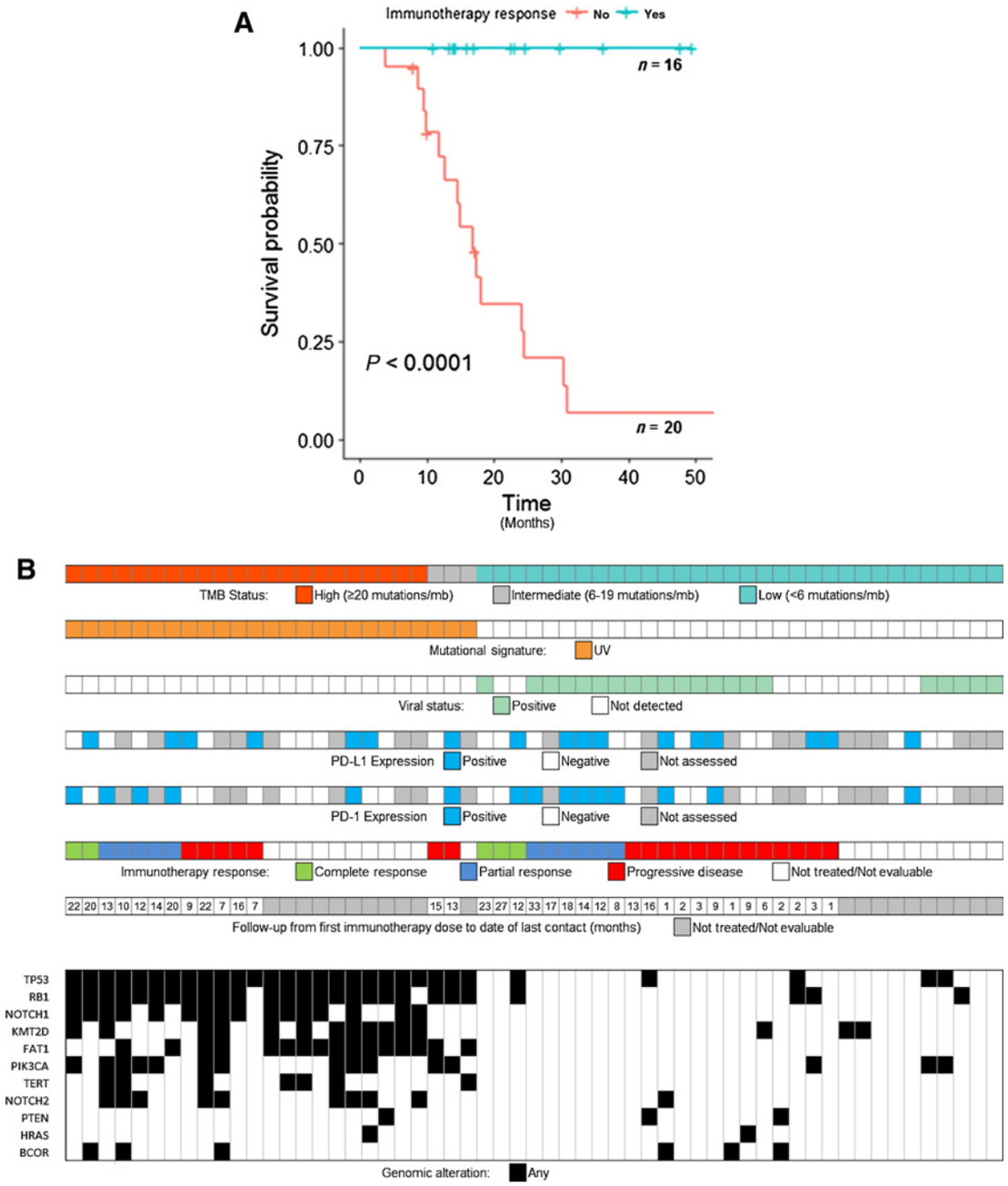

Figure 3.

Response to treatment with immune checkpoint inhibitors and patient survival. **A**, Kaplan–Meier plot of OS in immunotherapy responders versus those with progressive disease. Patients with favorable immunotherapy response have dramatically prolonged survival from the time of advanced/metastatic diagnosis compared with immunotherapy-treated patients without a good response. Patients were considered to be responders if they were assessed as having a CR, PR, or stable disease for at least 6 months. **B,** Relationship between tumor mutation burden, mutational signature, viral status (by NGS only), PD-L1 expression, PD-1 expression, response to therapy, and selected genomic alterations among 57 patients in clinical cohort.

specifically in the context of drug-resistant disease (4, 43, 48). Genomically, they are largely defined by mutationally or virally-abrogated *RB1* and *TP53* function, with upregulation of MYC activity, all features which are observed to be relevant in animal models as well (49). UV-driven MCC is characterized by a high TMB, mutation of *TP53* and *RB1*, a UV mutational signature, and absence of MCPyV DNA. It is most closely linked to SCLC, both of which are closely associated with exposure to the environmental carcinogens such as UV radiation and cigarette smoke, respectively (Fig. 2B). The MCPyV-positive/TMB-low subset is defined by a low TMB along with MCPyV DNA integration and is most closely associated with HPV and HHV-8-driven cancers as well as

Table 2. Clinical outcomes in immune checkpoint therapy–treated patients

	Response rate	*P* value
Molecular subtype		
UV-driven	50% (7/14)	0.63
Viral positive/TMB-low	41% (9/22)	
Line of therapy		
First	75% (9/12)	0.0066
Second	39% (5/13)	
Third or later	18% (2/11)	
PD-L1		
<1%	54% (7/13)	0.606
≥1%	43% (6/14)	
PD-1		
Negative	21% (3/14)	0.00598
Positive	77% (10/13)	
Prior radiation therapy		
Yes	59% (17/29)	0.60
No	43% (3/7)	

carcinoid tumors largely by virtue of their low mutational burdens (Fig. 2B). Pulmonary carcinoid tumors appear to be driven by mutations in chromatin modifiers (50), which may overlap with some functions of MCPyV small T-antigen, which has also been shown to interact with MYCL to drive oncogenic chromatin remodeling (46). Taken together, these data strongly suggest that many, if not all, neuroendocrine cancers may have genomic commonalities that portend common therapeutic approaches.

Despite a clear molecular delineation between the UV-driven and MCPyV-positive/TMB-low subtypes of MCC, both groups have a similar response rate to checkpoint inhibitor therapy (Fig. 3B). This finding is consistent with the results of previous clinical trials and is likely reflective of 2 distinct but dually effective mechanisms of response.(21, 22) Across multiple cancer types, a high TMB has been associated with increased likelihood of clinical benefit from immune checkpoint therapy, a finding attributed to a greater number of neoantigens that can be recognized by the immune system (51, 52). Indeed, many immune checkpoint inhibitors have demonstrated clinical benefit in cancer types with a generally high TMB, such as cutaneous melanoma and non-small cell lung cancer. However, in MCC frequent response to immune checkpoint therapy in MCPyV-positive cases has contributed to a response rate that exceeds what would be predicted by median TMB alone (53). Presumably, viral antigens provide an alternate source of immunogenicity in the TMB-low viral subgroup (54, 55).

Intriguingly, we were able to assess viral genomic integration in a subset of samples and show direct disruption of tumor suppressor genes such as *TP53* at some integration sites. Additional work is warranted to further characterize this potential mechanism of oncogenesis. One potential limitation of our study is that MCPyV-positivity was defined by detection of viral sequences utilizing off-target sequencing reads in an NGS-based assay. Although exploratory, our results provided proof of concept for this approach. Furthermore, confirmatory IHC in a subset of tumors supported the specificity of NGS-based viral detection. The TMB-low cases for which MCPyV sequences were not detected, are likely to be MCPyV-driven tumors for which viral sequences were undetectable by this method. If that is the case, our proportion of MCPyV-driven to UV-driven tumors was approximately 60:40, nearly identical to cohorts in recent clinical trials for advanced MCC (21, 22). Furthermore, the lack of an APOBEC mutational signature in the MCyPV-positive/TMB-low subset is notable with respect to how strong the APOBEC signature is in other viral-driven tumors, particularly HPV-associated tumors (56). Whole genome sequencing has also thus far failed to implicate APOBEC-mediated mutagenesis in MCC (57) perhaps suggesting that MCPyV can override APOBEC restriction of viral replication or a short latency between productive infection and tumor development. Nevertheless, the dichotomy between MCPyV-positive (NGS)/TMB-low cases and those with either a UV mutational signature or a high TMB in this large cohort demonstrates the presence of at least 2 major biologically distinct groups of MCC.

To our knowledge, our clinical review is the largest single-center immunotherapy experience for MCC in the literature to date and highlights several clinically relevant observations. First, we demonstrate that response to immunotherapy has a dramatic impact on survival for advanced MCC. This is in line with most recent updates from immunotherapy clinical trials in this disease (23, 24) and lends further evidence to the applicability of these results to the general MCC population. Crucially, we observed that the line of therapy in which immunotherapy was given has a dramatic effect on response rate. This result has been suggested previously by indirect comparison across clinical trials, although differences in trial design and cross-study comparisons precluded definitive conclusions. We believe that the significant decrease in immunotherapy response rate from first- to second- to third-line plus observed in our study and in light of previous trial results provides convincing evidence of this phenomenon. We therefore agree strongly with most current NCCN guidelines that immunotherapy should preferentially be utilized in the first-line setting for all eligible patients with advanced MCC. Although small in numbers, another important clinical observation from our study was that 0 of 4 patients who failed anti-PD-1/PD-L1 therapy had a successful response after switching to an alternate anti-PD-1/PD-L1 monotherapy. Patients for whom 1 anti-PD-1/PD-L1 agent has failed should therefore be offered alternate treatment, ideally on a clinical trial, rather than routinely switched to another anti-PD-1/PD-L1 agent.

In regards to other potential biomarkers of immunotherapy response, we found a statistically significant association between PD-1, but not PD-L1, positivity, and immunotherapy response. This finding corroborates and extends a previous finding that MCC from patients who responded to anti-PD-1 therapy showed higher densities of PD-1-positivity when compared with nonresponders (35) and warrants prospective validation.

In summary, this study represents the largest description of the genomic landscape of MCC. Although there are 2 distinct molecular subsets of this disease, interestingly, they exhibit similar response rates to checkpoint inhibitor therapy. In one of the largest clinical experiences to date with checkpoint inhibitor therapy use in this disease, a significant impact of line of therapy on checkpoint inhibitor response rate was noted.

Disclosure of Potential Conflicts of Interest

S. Sokol has ownership interests (including patents) in Foundation Medicine. G.M. Frampton has ownership interests (including patents) in Roche. V.A. Miller is an employee of Foundation Medicine and Revolution Medicines. L.A. Albacker has ownership interests (including patents) at Roche. H.L. McLeod has ownership interests (including patents) at Cancer Genetics and Interpares Biomedicine, reports receiving speakers bureau honoraria from Illumina and Genentech, and is a consultant/advisory board member for Pharmazam and Admera Health. Z. Eroglu is a consultant/advisory board member for Array and Regeneron. N.I. Khushalani has ownership interests (including patents) at

Bellicum Pharmaceuticals, Amarin Corp., Mazor Robotics, and TransEnteriz; is a consultant/advisory board member for Bristol-Myers Squibb, HUA, Merck, EMD Serono, Array, Regeneron, Immunocore, and Genentech; reports receiving commercial research grants to his institute from Bristol-Myers Squibb, Merck, HUYA Bioscience, GlaxoSmithKline, Amgen, Regeneron, Celgene, and Novartis; and has been on the Data and Safety Monitoring Board (DSMB) for AstraZeneca. V.K. Sondak is a consultant/advisory board member for Merck, Bristol-Myers Squibb, Regeneron, Pfizer, Novartis, Array, Genentech/Roche, and Polynoma. J.A. DeCaprio is a consultant/advisory board member for Merck Sharp & Dohme and reports receiving commercial research grants from Constellation Pharmaceuticals. K.Y. Tsai is a consultant/advisory board member for Merck. No potential conflicts of interest were disclosed by the other authors.

Authors' Contributions

Conception and design: T.C. Knepper, J.S. Russell, E.S. Sokol, G.M. Frampton, H.L. McLeod, V.K. Sondak, J.A. DeCaprio, K.Y. Tsai, A.S. Brohl
Development of methodology: T.C. Knepper, M. Montesion, E.S. Sokol, G.M. Frampton, L.A. Albacker, J.A. DeCaprio, K.Y. Tsai
Acquisition of data (provided animals, acquired and managed patients, provided facilities, etc.): J.S. Russell, E.S. Sokol, G.M. Frampton, H.L. McLeod, N.I. Khushalani, J.L. Messina, K.Y. Tsai, A.S. Brohl
Analysis and interpretation of data (e.g., statistical analysis, biostatistics, computational analysis): T.C. Knepper, M. Montesion, G.M. Frampton, V.A. Miller, L.A. Albacker, H.L. McLeod, V.K. Sondak, M.J. Schell, J.A. DeCaprio, K.Y. Tsai, A.S. Brohl
Writing, review, and/or revision of the manuscript: T.C. Knepper, M. Montesion, J.S. Russell, E.S. Sokol, V.A. Miller, L.A. Albacker, H.L. McLeod, Z. Eroglu, N.I. Khushalani, V.K. Sondak, J.L. Messina, M.J. Schell, J.A. DeCaprio, K.Y. Tsai, A.S. Brohl
Administrative, technical, or material support (i.e., reporting or organizing data, constructing databases): T.C. Knepper, V.A. Miller, H.L. McLeod, V.K. Sondak, K.Y. Tsai, A.S. Brohl
Study supervision: J.A. DeCaprio, K.Y. Tsai, A.S. Brohl

Acknowledgments

This work has been supported in part by the Tissue Core Facility at the H. Lee Moffitt Cancer Center & Research Institute, an NCI designated Comprehensive Cancer Center (P30-CA076292), and the Campbell Family Foundation (to K.Y. Tsai). This work was funded in part by HHS | NIH | National Cancer Institute (NCI) RO1CA63113, RO1CA173023, and PO1CA050661, the DFCI Helen Pappas Merkel Cell Research Fund, and the Claudia Adams Barr Program in Cancer Research to J.A. DeCaprio. T.C. Knepper was supported by the NCI of the NIH under an LRP award related to this work. Foundation Medicine, Inc., performed the genomic sequencing in the commercial setting and conducted the bioinformatics analysis, but did not provide direct funding for research support.

The costs of publication of this article were defrayed in part by the payment of page charges. This article must therefore be hereby marked *advertisement* in accordance with 18 U.S.C. Section 1734 solely to indicate this fact.

Received December 19, 2018; revised March 27, 2019; accepted July 26, 2019; published first August 9, 2019.

References

1. van der Zwan JM, Trama A, Otter R, Larranaga N, Tavilla A, Marcos-Gragera R, et al. Rare neuroendocrine tumours: results of the surveillance of rare cancers in Europe project. Eur J Cancer 2013;49:2565–78.
2. Fitzgerald TL, Dennis S, Kachare SD, Vohra NA, Wong JH, Zervos EE. Dramatic increase in the incidence and mortality from Merkel cell carcinoma in the United States. Am Surg 2015;81:802–6.
3. Youlden DR, Soyer HP, Youl PH, Fritschi L, Baade PD. Incidence and survival for Merkel cell carcinoma in Queensland, Australia, 1993–2010. JAMA Dermatol 2014;150:864–72.
4. Becker JC, Stang A, DeCaprio JA, Cerroni L, Lebbe C, Veness M, et al. Merkel cell carcinoma. Nat Rev Dis Primers 2017;3:17077.
5. Feng H, Shuda M, Chang Y, Moore PS. Clonal integration of a polyomavirus in human Merkel cell carcinoma. Science 2008;319:1096–100.
6. Santos-Juanes J, Fernandez-Vega I, Fuentes N, Galache C, Coto-Segura P, Vivanco B, et al. Merkel cell carcinoma and Merkel cell polyomavirus: a systematic review and meta-analysis. Br J Dermatol 2015;173:42–9.
7. Paik JY, Hall G, Clarkson A, Lee L, Toon C, Colebatch A, et al. Immunohistochemistry for Merkel cell polyomavirus is highly specific but not sensitive for the diagnosis of Merkel cell carcinoma in the Australian population. Hum Pathol 2011;42:1385–90.
8. Sihto H, Kukko H, Koljonen V, Sankila R, Bohling T, Joensuu H. Clinical factors associated with Merkel cell polyomavirus infection in Merkel cell carcinoma. J Natl Cancer Inst 2009;101:938–45.
9. Schrama D, Peitsch WK, Zapatka M, Kneitz H, Houben R, Eib S, et al. Merkel cell polyomavirus status is not associated with clinical course of Merkel cell carcinoma. J Invest Dermatol 2011;131:1631–8.
10. Moshiri AS, Doumani R, Yelistratova L, Blom A, Lachance K, Shinohara MM, et al. Polyomavirus-negative Merkel cell carcinoma: a more aggressive subtype based on analysis of 282 cases using multimodal tumor virus detection. J Invest Dermatol 2017;137:819–27.
11. Miller NJ, Bhatia S, Parvathaneni U, Iyer JG, Nghiem P. Emerging and mechanism-based therapies for recurrent or metastatic Merkel cell carcinoma. Curr Treat Options Oncol 2013;14:249–63.
12. Lemos BD, Storer BE, Iyer JG, Phillips JL, Bichakjian CK, Fang LC, et al. Pathologic nodal evaluation improves prognostic accuracy in Merkel cell carcinoma: analysis of 5823 cases as the basis of the first consensus staging system. J Am Acad Dermatol 2010;63:751–61.
13. Allen PJ, Bowne WB, Jaques DP, Brennan MF, Busam K, Coit DG. Merkel cell carcinoma: prognosis and treatment of patients from a single institution. J Clin Oncol 2005;23:2300–9.
14. Santamaria-Barria JA, Boland GM, Yeap BY, Nardi V, Dias-Santagata D, Cusack JC, Jr. Merkel cell carcinoma: 30-year experience from a single institution. Ann Surg Oncol 2013;20:1365–73.
15. Toker C. Trabecular carcinoma of the skin. Arch Dermatol 1972;105:107–10.
16. Sharma D, Flora G, Grunberg SM. Chemotherapy of metastatic Merkel cell carcinoma: case report and review of the literature. Am J Clin Oncol 1991;14:166–9.
17. Voog E, Biron P, Martin JP, Blay JY. Chemotherapy for patients with locally advanced or metastatic Merkel cell carcinoma. Cancer 1999;85:2589–95.
18. Tai PT, Yu E, Winquist E, Hammond A, Stitt L, Tonita J, et al. Chemotherapy in neuroendocrine/Merkel cell carcinoma of the skin: case series and review of 204 cases. J Clin Oncol 2000;18:2493–9.
19. Iyer JG, Blom A, Doumani R, Lewis C, Tarabadkar ES, Anderson A, et al. Response rates and durability of chemotherapy among 62 patients with metastatic Merkel cell carcinoma. Cancer Med 2016;5:2294–301.
20. Nghiem P, Kaufman HL, Bharmal M, Mahnke L, Phatak H, Becker JC. Systematic literature review of efficacy, safety and tolerability outcomes of chemotherapy regimens in patients with metastatic Merkel cell carcinoma. Future Oncol 2017;13:1263–79.
21. Nghiem PT, Bhatia S, Lipson EJ, Kudchadkar RR, Miller NJ, Annamalai L, et al. PD-1 blockade with pembrolizumab in advanced Merkel cell carcinoma. N Engl J Med 2016;374:2542–52.
22. Kaufman HL, Russell J, Hamid O, Bhatia S, Terheyden P, D'Angelo SP, et al. Avelumab in patients with chemotherapy-refractory metastatic Merkel cell carcinoma: a multicentre, single-group, open-label, phase 2 trial. Lancet Oncol 2016;17:1374–85.
23. Kaufman HL, Russell JS, Hamid O, Bhatia S, Terheyden P, D'Angelo SP, et al. Updated efficacy of avelumab in patients with previously treated metastatic Merkel cell carcinoma after $\geq$1 year of follow-up: JAVELIN Merkel 200, a phase 2 clinical trial. J Immunother Cancer 2018;6:7.
24. Nghiem P, Bhatia S, Lipson EJ, Sharfman WH, Kudchadkar RR, Friedlander PA, et al. Durable tumor regression and overall survival (OS) in patients

with advanced Merkel cell carcinoma (aMCC) receiving pembrolizumab as first-line therapy. J Clin Oncol 2018;36:9506.
25. Harms PW, Vats P, Verhaegen ME, Robinson DR, Wu YM, Dhanasekaran SM, et al. The distinctive mutational spectra of polyomavirus-negative Merkel cell carcinoma. Cancer Res 2015;75:3720–7.
26. Wong SQ, Waldeck K, Vergara IA, Schroder J, Madore J, Wilmott JS, et al. UV-associated mutations underlie the etiology of MCV-negative Merkel cell carcinomas. Cancer Res 2015;75:5228–34.
27. Goh G, Walradt T, Markarov V, Blom A, Riaz N, Doumani R, et al. Mutational landscape of MCPyV-positive and MCPyV-negative Merkel cell carcinomas with implications for immunotherapy. Oncotarget 2016;7:3403–15.
28. Gonzalez-Vela MD, Curiel-Olmo S, Derdak S, Beltran S, Santibanez M, Martinez N, et al. Shared oncogenic pathways implicated in both virus-positive and UV-induced Merkel cell carcinomas. J Invest Dermatol 2017; 137:197–206.
29. Carter MD, Gaston D, Huang WY, Greer WL, Pasternak S, Ly TY, et al. Genetic profiles of different subsets of Merkel cell carcinoma show links between combined and pure MCPyV-negative tumors. Hum Pathol 2018; 71:117–25.
30. Frampton GM, Fichtenholtz A, Otto GA, Wang K, Downing SR, He J, et al. Development and validation of a clinical cancer genomic profiling test based on massively parallel DNA sequencing. Nat Biotechnol 2013;31: 1023–31.
31. Chalmers ZR, Connelly CF, Fabrizio D, Gay L, Ali SM, Ennis R, et al. Analysis of 100,000 human cancer genomes reveals the landscape of tumor mutational burden. Genome Med 2017;9:34.
32. Sun JX, He Y, Sanford E, Montesion M, Frampton GM, Vignot S, et al. A computational approach to distinguish somatic vs. germline origin of genomic alterations from deep sequencing of cancer specimens without a matched normal. PLoS Comput Biol 2018;14:e1005965.
33. Zehir A, Benayed R, Shah RH, Syed A, Middha S, Kim HR, et al. Mutational landscape of metastatic cancer revealed from prospective clinical sequencing of 10,000 patients. Nat Med 2017;23:703–13.
34. Alexandrov LB, Nik-Zainal S, Wedge DC, Aparicio SA, Behjati S, Biankin AV, et al. Signatures of mutational processes in human cancer. Nature 2013;500:415–21.
35. Giraldo NA, Nguyen P, Engle EL, Kaunitz GJ, Cottrell TR, Berry S, et al. Multidimensional, quantitative assessment of PD-1/PD-L1 expression in patients with Merkel cell carcinoma and association with response to pembrolizumab. J Immunother Cancer 2018;6:99.
36. Lydersen S, Fagerland MW, Laake P. Recommended tests for association in 2 x 2 tables. Stat Med 2009;28:1159–75.
37. George J, Lim JS, Jang SJ, Cun Y, Ozretic L, Kong G, et al. Comprehensive genomic profiles of small cell lung cancer. Nature 2015;524:47–53.
38. Li YY, Hanna GJ, Laga AC, Haddad RI, Lorch JH, Hammerman PS. Genomic analysis of metastatic cutaneous squamous cell carcinoma. Clin Cancer Res 2015;21:1447–56.
39. Pickering CR, Zhou JH, Lee JJ, Drummond JA, Peng SA, Saade RE, et al. Mutational landscape of aggressive cutaneous squamous cell carcinoma. Clin Cancer Res 2014;20:6582–92.
40. Wang NJ, Sanborn Z, Arnett KL, Bayston LJ, Liao W, Proby CM, et al. Loss-of-function mutations in Notch receptors in cutaneous and lung squamous cell carcinoma. Proc Natl Acad Sci U S A 2011;108:17761–6.
41. South AP, Purdie KJ, Watt SA, Haldenby S, den Breems N, Dimon M, et al. NOTCH1 mutations occur early during cutaneous squamous cell carcinogenesis. J Invest Dermatol 2014;134:2630–8.
42. Chitsazzadeh V, Coarfa C, Drummond JA, Nguyen T, Joseph A, Chilukuri S, et al. Cross-species identification of genomic drivers of squamous cell carcinoma development across preneoplastic intermediates. Nat Commun 2016;7:12601.
43. McConkey DJ, Choi W. Molecular subtypes of bladder cancer. Curr Oncol Rep 2018;20:77.
44. Spratt DE, Zumsteg ZS, Feng FY, Tomlins SA. Translational and clinical implications of the genetic landscape of prostate cancer. Nat Rev Clin Oncol 2016;13:597–610.
45. Paulson KG, Lemos BD, Feng B, Jaimes N, Penas PF, Bi X, et al. Array-CGH reveals recurrent genomic changes in Merkel cell carcinoma including amplification of L-Myc. J Invest Dermatol 2009;129:1547–55.
46. Cheng J, Park DE, Berrios C, White EA, Arora R, Yoon R, et al. Merkel cell polyomavirus recruits MYCL to the EP400 complex to promote oncogenesis. PLoS Pathog 2017;13:e1006668.
47. Al-Rohil RN, Tarasen AJ, Carlson JA, Wang K, Johnson A, Yelensky R, et al. Evaluation of 122 advanced-stage cutaneous squamous cell carcinomas by comprehensive genomic profiling opens the door for new routes to targeted therapies. Cancer 2016;122:249–57.
48. Aggarwal R, Huang J, Alumkal JJ, Zhang L, Feng FY, Thomas GV, et al. Clinical and genomic characterization of treatment-emergent small-cell neuroendocrine prostate cancer: a multi-institutional prospective study. J Clin Oncol 2018;36:2492–503.
49. Rickman DS, Beltran H, Demichelis F, Rubin MA. Biology and evolution of poorly differentiated neuroendocrine tumors. Nat Med 2017;23:1–10.
50. Fernandez-Cuesta L, Peifer M, Lu X, Sun R, Ozretic L, Seidal D, et al. Frequent mutations in chromatin-remodelling genes in pulmonary carcinoids. Nat Commun 2014;5:3518.
51. Rizvi NA, Hellmann MD, Snyder A, Kvistborg P, Makarov V, Havel JJ, et al. Cancer immunology. Mutational landscape determines sensitivity to PD-1 blockade in non-small cell lung cancer. Science 2015;348: 124–8.
52. Hellmann MD, Ciuleanu TE, Pluzanski A, Lee JS, Otterson GA, Audigier-Valette C, et al. Nivolumab plus ipilimumab in lung cancer with a high tumor mutational burden. N Engl J Med 2018;378:2093–104.
53. Yarchoan M, Hopkins A, Jaffee EM. Tumor mutational burden and response rate to PD-1 inhibition. N Engl J Med 2017;377:2500–1.
54. Topalian SL, Taube JM, Anders RA, Pardoll DM. Mechanism-driven biomarkers to guide immune checkpoint blockade in cancer therapy. Nat Rev Cancer 2016;16:275–87.
55. El-Khoueiry AB, Sangro B, Yau T, Crocenzi TS, Kudo M, Hsu C, et al. Nivolumab in patients with advanced hepatocellular carcinoma (CheckMate 040): an open-label, non-comparative, phase 1/2 dose escalation and expansion trial. Lancet 2017;389:2492–502.
56. Roberts SA, Lawrence MS, Klimczak LJ, Grimm SA, Fargo D, Stojanov P, et al. An APOBEC cytidine deaminase mutagenesis pattern is widespread in human cancers. Nat Genet 2013;45:970–6.
57. Starrett GJ, Marcelus C, Cantalupo PG, Katz JP, Cheng J, Akagi K, et al. Merkel cell polyomavirus exhibits dominant control of the tumor genome and transcriptome in virus-associated merkel cell carcinoma. MBio 2017;8. doi: 10.1128/mBio.02079–16.